

Tacticity of poly(butyl- α -cyanoacrylate) chains in nanoparticles: NMR spectroscopy and DFT calculations

Nadezhda Markova · Galya Ivanova ·
Venelin Enchev · Margarita Simeonova

Received: 14 May 2011 / Accepted: 6 December 2011 / Published online: 22 December 2011
© Springer Science+Business Media, LLC 2011

Abstract NMR spectroscopy and quantum chemical calculations were applied for structural characterization and determination of the preferred stereochemical sequence distribution of the monomer units in the homopolymer chains of poly(butyl- α -cyanoacrylate) nanoparticles. The stereochemical sequence distribution of the monomer units was defined by analysis of their high-resolution 1D ^1H and ^{13}C NMR and 2D J -resolved, $^1\text{H}/^{13}\text{C}$ HSQC and $^1\text{H}/^{13}\text{C}$ HMBC NMR spectra. The results were verified by employment of B3LYP/6-31G(d) calculations and are consistent with the preferred tendency of polymer chains of PBCN to adopt syndiotactic placements. The proton and carbon chemical shielding were calculated at BPW91/6-31+G(2d,p) level using the GIAO approach and B3LYP/6-31G(d) optimized geometry.

Keywords NMR · DFT · Stereochemistry · Poly(butyl- α -cyanoacrylate) · Nanoparticles

Introduction

In recent years, there has been intensive research on the development of novel multifunctional nanoparticles for biomedical and diagnostic applications [1–3]. The main challenge in the design of drug delivery systems is to obtain a higher therapeutic effect with minimal toxicity, and the protection of the incorporated drugs from premature deactivation before reaching the desired site of action.

Poly(alkyl- α -cyanoacrylate) (PACA) nanoparticles have been developed as colloidal drug carriers intended for an intralysosomal drug delivery by Couvreur et al. [4]. This specific function of the nanoparticles is facilitated by their susceptibility to degradation by lysosomal enzymes [5–7] such as carboxylic ester hydrolases. The possibility of lysosomal degradation is very important in relation to the biocompatibility of these polymers and could be a key to their successful functioning as drug delivery systems [8]. It was shown that PACA nanoparticles undergo enzymatic ester side chain hydrolysis yielding a respective primary alkylalcohol and water-soluble poly(- α -cyanoacetic) acid [5–7, 9, 10], which could be eliminated in vivo by kidney filtration. Nowadays, the ester side chain hydrolysis is assumed as the main degradation route of PACA nanoparticles in vivo [9]. In the literature, there is a number of publications about the control of the length of alkyl side chain over the rate of polymerization and biodegradation of poly(alkyl- α -cyanoacrylates) [11–14]. Surprisingly, to the best of our knowledge, there is no data about the influence of polymer microstructure on the rate of degradation that could connect the length of alkyl side chains and microstructure of PACA. This seems strange because the accessibility of the ester side bonds of poly(alkyl- α -cyanoacrylates) for the active site of hydrolytic enzymes

N. Markova · V. Enchev (✉)
Institute of Organic Chemistry, Bulgarian Academy of Sciences,
1113 Sofia, Bulgaria
e-mail: venelin@orgchm.bas.bg

G. Ivanova (✉)
REQUIMTE, Departamento de Química, Faculdade de Ciências,
Universidade do Porto, 4169-007 Porto, Portugal
e-mail: galya.ivanova@fc.up.pt

M. Simeonova
Department of Polymer Engineering, University of Chemical
Technology and Metallurgy, 8 Kliment Ohridski Blvd.,
1756 Sofia, Bulgaria

should be closely related with this microstructure and thereby could be a key factor for the rate of degradation and release characteristics of these polymers.

It is well established that chemical and physical properties of polymers, such as biodegradability, strength of adhesion, polymer hydrophilic/hydrophobic properties, and biocompatibility are directly related to their chemical structure and stereochemical sequence distribution. The knowledge of the chemical composition and tacticity of polymers and influence of these parameters on various polymer properties is important for the biomedical and diagnostic applications of alkyl- α -cyanoacrylate-based polymers. Nuclear magnetic resonance (NMR) spectroscopy is one of the most efficient and powerful experimental methods for evaluation of structural and stereochemical characteristics of polymers [15]. NMR spectroscopy offers the chance to monitor chemical composition and distribution of monomer units of copolymers as well as the stereochemical sequence distribution of the monomer units in homopolymers.

The aim of the work is to find all possible sequences with relation to COOBu and CN groups' position to main chain in the tetramers of butyl- α -cyanoacrylate. We report a structural study of poly(butyl- α -cyanoacrylate), based on NMR spectroscopy and theoretical calculations. The structural characterization and preferred stereochemical sequence distribution of the monomer units in the homopolymer chains of poly(butyl- α -cyanoacrylate) were studied by ^1H and ^{13}C NMR spectroscopy employing one- and two-dimensional NMR techniques and the results have been verified by quantum chemical calculations.

Experimental and computational details

Materials

The monomer, *n*-butyl- α -cyanoacrylate (*n*-BCA) was purchased from the Research Centre for Specialty Polymers, Bulgaria. Dextran 40 (mol. wt. 40,000 g/mol) was obtained from Pharmachim (Bulgaria) and citric acid as monohydrate from Aldrich. Other chemicals were of laboratory grade purity and used as obtained.

Preparation and characterization of nanoparticles

Poly(butyl- α -cyanoacrylate) nanoparticles (PBCN) were produced by in situ anionic polymerization, accomplished as a dispersion polymerization process. The monomer, butyl- α -cyanoacrylate (130.7 mmol/L) was carefully dripped to an aqueous polymerization medium, containing citric acid (9.5 mmol/L) as an acidifying agent and dextran 40 (molecular weight 40,000 g/mol) at concentration of

0.2 mmol/L) as a steric colloidal stabilizer. Polymerization was carried out for 3 h at room temperature with continuous magnetic stirring. The resulting colloidal polymer suspension was then adjusted to pH 7 using 1N sodium hydroxide.

The diameter of PBCN was measured by photon correlation spectroscopy (PCS) using a laser beam scattered at 173° and temperature 25°C (Zetasizer ZS, Malvern Instruments, England). Zeta-potential was measured by laser Doppler electrophoresis on the same apparatus at 25°C . Their molecular weight was determined by gel permeation chromatography (GPC, Waters 150 GPC system fitted with refractive index (Waters R401) in THF.

To perform the GPC and NMR analyses, the intact aqueous colloidal suspension of PBCN was filtered over a $0.1\text{-}\mu\text{m}$ pore-sized VC membrane (Millipore, England). After filtration, the moist nanoparticles mass was transferred from the filtration membrane to a small plastic test tube, dried under vacuum, and was kept in a vacuum desiccator over P_2O_5 .

NMR spectroscopy

The NMR spectra were recorded on a Bruker AvanceIII 400, operating at 400.15 MHz for protons and 100.62 MHz for carbons, equipped with pulse gradient units, capable of producing magnetic field pulsed gradients in the *z*-direction of 50.0 G/cm. All NMR spectra were acquired in $\text{DMSO-}d_6$ as a solvent at a temperature of 300 K. The solvent resonance peak at 2.49 ppm for proton and 39.5 ppm for carbon were used as a chemical shift reference. Standard 1D ^1H NMR experiments with 30° pulses, acquisition time 16.4 s, relaxation delay 1 s, 64 transients of a spectral width of 2,000 Hz were collected into 32 K time domain points. Following acquisition parameters were used for the full range broad-band proton decoupled ^{13}C and DEPT NMR spectra: a pulse width of 8 μs , an acquisition time of 2 s, a relaxation delay of 2 s, a spectral width of 16,000 Hz, 64 K time domain points, and 10,000 transients were collected. For the purpose of quantitative analysis, ^{13}C NMR spectra were recorded using the inverse-gated decoupling technique, with the decoupler off except during the acquisition time, in order to obtain ^{13}C NMR spectra decoupled from the protons but without Nuclear Overhauser Enhancement (NOE). More than 5,000 scans were normally accumulated to achieve a good signal to noise ratio necessarily for the quantitative analysis. The relative intensities of the carbon resonance signals in ^{13}C NMR spectra were obtained by deconvolution of the spectral lines using the standard Bruker software and Lorentzian curves.

Two-dimensional $^1\text{H}/^1\text{H}$ correlation spectra (COSY), gradient-selected $^1\text{H}/^{13}\text{C}$ heteronuclear single quantum

coherence (HSQC), and $^1\text{H}/^{13}\text{C}$ heteronuclear multiple bond coherence (HMBC) spectra were acquired using the standard Bruker software. Magnitude-mode ge-2D-COSY spectra with double quantum filter, gradient pulses for selection, gradient ratio 16:12:40, and ^1H J -resolved NMR experiments were recorded at relaxation delay 2 s, a spectral width of 2,000 Hz, a total 2K data points in F_2 , and 512 data points in F_1 for COSY and 128 for J -resolved spectra, FT size $2\text{K} \times 2\text{K}$.

Two-dimensional $^1\text{H}/^{13}\text{C}$ HSQC and $^1\text{H}/^{13}\text{C}$ HMBC spectra were obtained using the standard Bruker software. 2D $^1\text{H}/^{13}\text{C}$ HSQC experiments were carried out with a spectral width of ca. 2,000 Hz for ^1H and 8,000 Hz for ^{13}C , relaxation delay 1.5 s, FT size $2\text{K} \times 1\text{K}$. $^1\text{H}/^{13}\text{C}$ HMBC spectra with a spectral width of 16,000 Hz in the carbon dimension and 1,600 Hz in the proton dimension were recorded and typical acquisition parameters: 90° pulses for protons and carbons, 7 and 12.5 μs , respectively, a relaxation delay of 1.5 s, 512 increments and an FT size of $4\text{K} \times 2\text{K}$.

Computational details

Eight tetramers (SSRS, SRSS, RRSS, SRSR, RRRS, SRRS, RRRR, SRRR) corresponding to the eight tetrads (*rrr*, *mrm*, *rrm*, *mrr*, *rmr*, *mmr*, *rrmm*, *mmmm*) of poly(butyl- α -cyanoacrylate) were considered. Geometry optimization of these structures was carried out at two different computational levels: semi-empirical PM3 method [16] and DFT—the hybrid B3LYP functional which combines the three-parameter exchange functional of Becke [17] with the LYP correlation one [18] using 6-31G(d) basis set. The calculations were carried out without symmetry constraints by the gradient procedure. A gradient convergence threshold of 1×10^{-4} hartree Bohr $^{-1}$ was used. All calculations were done using the computational chemistry program Firefly [19].

The proton and carbon chemical shielding were calculated with different functionals (B3LYP, OLYP, OPBE, BPW91, B3PW91) and basis sets (MidiX, 6-31G(d), 6-31+G(d)) using the gauge-including atomic orbitals (GIAO) approach [20, 21] and B3LYP/6-31G(d) optimized geometry. The closest to experimental data results were obtained at BPW91/6-31+G(2d,p) level. BPW91 uses the Becke [17] exchange functional and Perdew and Wang's [22] gradient-corrected correlation functional. The including of the solvent as dielectric (polarizable continuum model) in GIAO NMR calculations was used to estimate the effect of the medium (DMSO) on the chemical shifts of the poly(methyl- α -cyanoacrylate) tetramers because of computational reasons. In order to compare with the experimental data, the calculated absolute shieldings were transformed to chemical shifts using the reference

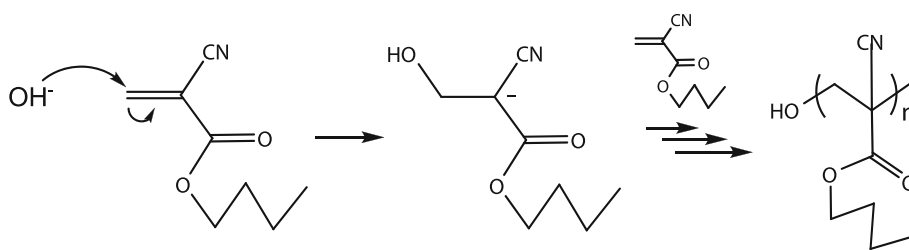
compound tetramethylsilane (TMS): $\delta = \delta_{\text{calc}}(\text{TMS}) - \delta_{\text{calc}}$. Both $\delta_{\text{calc}}(\text{TMS})$ and δ_{calc} were evaluated with the same method and basis set. The NMR calculations were carried out using GAUSSIAN 09 program package [23].

Results and discussion

One of the most frequently used methods to produce PACA nanoparticles is based on the in situ polymerization of monomers in various media. Depending on the presence or not of an emulsifier, two types of polymerization processes are adopted for the preparation of polymeric nanoparticles: dispersion polymerization and emulsion polymerization. Due to the presence of the two powerful electron-withdrawing groups [the ester ($-\text{COOBU}$) and cyano ($-\text{CN}$)] in the α -carbon of the double bond, *n*-BCA monomer exhibits a remarkable reactivity toward nucleophiles (OH, NH, etc.), resulting in a very high-polymerization rate. In fact, alkyl- α -cyanoacrylate monomers are able to polymerize extremely rapidly in the presence of moisture or traces of basic components. PBCN were prepared by in situ anionic polymerization of *n*-BCA monomer accomplished as a dispersion polymerization process. The polymerization was initiated by the hydroxyl ions of water, while the elongation of the polymer chains occurs according to an anionic polymerization mechanism (Scheme 1). The anionic polymerization in the aqueous medium that generates simultaneously initiator (OH^-) and terminated agent (H^+) is mainly controlled by the pH of the system. This is the reason for the presence of citric acid in the polymerization medium. The polymer is formed in the continuous aqueous phase (in which it is insoluble) and precipitates into a new particulate phase stabilized by the polymeric stabilizer (dextran 40). Nanoparticles are formed by the aggregation of growing polymer chains precipitating from the continuous phase when these chains exceed a critical chain length [24]. The diameter of PBCN was 154.1 nm (monomodal narrow size distribution, polydispersity index 0.075) as measured by PCS, while Zeta-potential was -4.57 ± 4.60 mV as measured by electrophoresis. Their molecular weight as determined by GPC was 1,083.

Butyl- α -cyanoacrylate-based polymers are chiral structures with asymmetric centers positioned at the main-chain quaternary carbons. The microstructure of the polymer is dependent on the stereochemical configuration and arrangement of the monomer units into the polymer chains. An assembly of a small number of monomer units within a macromolecular chain is called sequence and the first terms of the series of sequences are referred to as dyad, triad, tetrad, and so forth. Tacticity reflects the existence of a relative configurational regularity of successive monomeric units along the macromolecular chain. The configurational

Scheme 1 Spontaneous anionic polymerization of *n*-butyl- α -cyanoacrylate monomer in an aqueous medium



and tactic arrangement of sequences can be described at triad–tetrad level using the two configurational possibilities offered by a dyad [25]. If the dyad consists of two identically oriented units, the dyad is called a meso dyad (*m*). If the dyad consists of units oriented in opposition, the dyad is called a racemo dyad (*r*). In the case of poly(butyl- α -cyanoacrylate), a meso dyad is one in which the *n*-butoxycarbonyl chains are oriented on the same side of the polymer backbone and the methylene protons are not in chemically equivalent environments. On the other hand, in the *r* dyad the two methylene protons have an identical environment due to the opposite orientation of the equivalent substituents with respect to the polymer backbone. The possible triad and tetrad arrangements of the monomer units of poly(butyl- α -cyanoacrylate) based on the two configurational possibilities of dyads are presented schematically on Scheme 2.

Thus, the meso–meso (*mm*) triad contains only meso (*m*) dyads, the racemo–racemo (*rr*) triad contains only racemo (*r*) dyads and the meso–racemo dyad contains one *m* and one *r* dyad. The presented tetrad structures evidence different molecular symmetry. The tetrads *rrr* and *mrm* exhibit C_2 point group symmetry, while *rmr* and *mmm* show C_s point group symmetry. However, the other four tetrads (*rrm*, *mrr*, *mmr*, *rrm*) are asymmetric in point group C_1 . An equivalence of the methylene protons of the main polymer chains of *rrr* and *mrm* tetrads and non-equivalence of those belonging to the other tetrads should be expected.

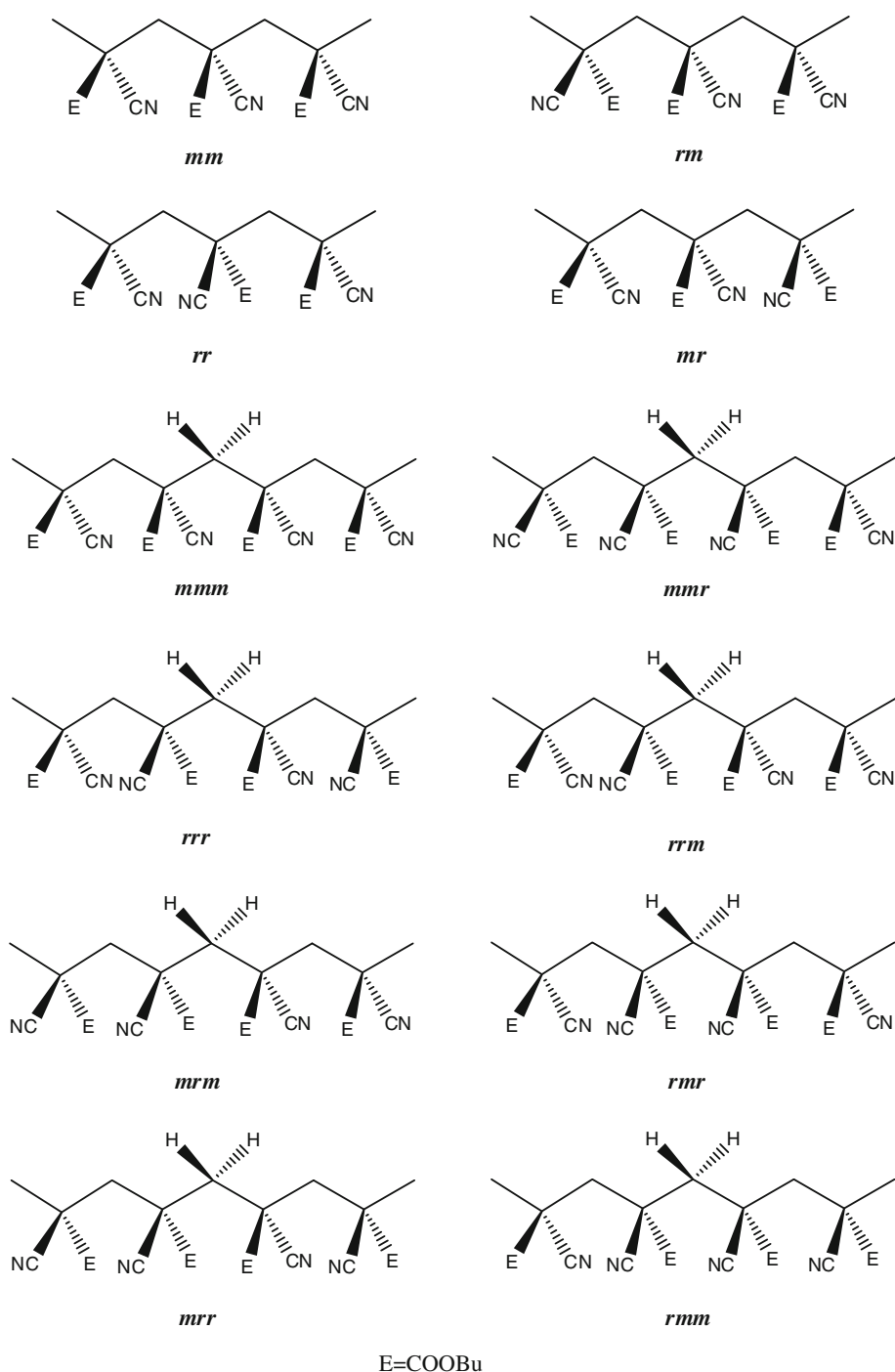
The structural characterization and estimation of the preferred stereochemical sequence distribution of the monomer units in the homopolymer chains of PBCN were studied by ^1H and ^{13}C NMR spectroscopy employing one- and two-dimensional NMR techniques. For a description of the monomer sequence distribution and their relative stereochemical configuration, it was taken into a consideration the possible arrangement of the monomer units in terms of triads and tetrads distribution. The types of triads and tetrads with different relative configurational structure were distinguished on the basis of *m* and *r* dyads, taking into account the relative configurations and consequently the immediate neighbors of stereosensitive sites under consideration (see below). It was considered that the methylene protons of the main polymer chains in *r* dyads

have the same chemical environments and therefore the same NMR resonance frequencies. However, in *m* dyads these protons are not in chemically equivalent environments and should display two different resonance frequencies, producing two different NMR signals. The existence of different triads and tetrads arrangement of the monomer units in the homopolymer chains results in an additional splitting of the resonance signals corresponding to each type of dyad. Stereochemical structures of tetramers representing the possible tetrad structures are shown on Fig. 1.

The assignment of the ^1H and ^{13}C resonances in the spectra of PBCN was based on the analysis of the one- (1D: ^1H , ^{13}C , DEPT) and two-dimensional (2D: $^1\text{H}/^1\text{H}$ COSY, *J*-resolved, $^1\text{H}/^{13}\text{C}$ HSQC and HMBC) NMR spectroscopic data. The ^1H NMR spectra were found to be much less informative than ^{13}C NMR spectra (Fig. 2).

The assignment of the resonance signals for triad and tetrad sequence distribution was achieved by analysis of the signals of OCH_2 (66 ppm) in ^{13}C NMR spectra and CH_2 of the main polymer chains in ^{13}C (42–45 ppm) and ^1H (2.40–2.80 ppm) NMR spectra. Proton NMR spectrum of PBCN shows broad, complex, overlapping resonance signals at 0.88, 1.39, 1.62, 4.12, and 2.59 ppm, corresponding to the protons belonging to the *n*-butoxycarbonyl group and those of methylene protons from the main polymer chain, respectively (Fig. 2). The complexity of the spectrum arises from the ^1H – ^1H scalar couplings and overlap of the signals belonging to protons of different stereoisomeric sequences in the polymer chains. The signals of CH_2 protons of the main polymer chains appeared as broad and complex multiplet in ^1H NMR spectrum of PBCN. The assignment of the resonance signals of the tetrad sequences was performed by analysis of $^1\text{H}/^1\text{H}$ COSY and *J*-resolved spectra. The results have confirmed the coexistence of different monomer sequence distribution with respect to their stereochemical configuration. The resonance signals at 2.58 and 2.69 ppm do not show coupling patterns in $^1\text{H}/^1\text{H}$ COSY and *J*-resolved spectra and were attributed to the methylene protons of *rrr* and *mrm* tetrads, respectively, where the both protons appear to be equivalent. Coupling patterns were observed between signals at 2.5–2.6 and 2.6–2.8 ppm of $^1\text{H}/^1\text{H}$ COSY spectra and were attributed to the methylene protons of the six C_s

Scheme 2 Schematic presentation of the possible triad and tetrad monomer sequences arrangement of poly(butyl- α -cyanoacrylate)



symmetric tetrads: *mmm*, *mmr*, *rrm*, *rrr*, *mrr*, and *rmr*. The analysis of *J*-resolved spectra has confirmed the existence of four couples of resonances (2.54/2.77, 2.63/2.69, 2.65/2.69, and 2.71/2.77 ppm) with non-equivalent methylene protons in strong germinal spin–spin coupling (Fig. 3).

A splitting of the resonance signals in the high-resolution ^{13}C NMR spectra of the PBCN was clearly observed (Fig. 2), due to the different stereochemical configuration

and arrangement of the monomer units into the polymer chains and variations in the length of the macromolecules. The assignment of the ^{13}C NMR resonance signals for triad and tetrad sequence distribution was obstructed due to overlap of the signals of the methylene and quaternary carbons of the main polymer chains. To avoid this complication and obtain the resonance assignment of the triad and tetrad sequence distribution in ^{13}C NMR spectrum of PBCN, we have employed high-resolution DEPT, $^1\text{H}/^{13}\text{C}$

Fig. 1 Eight B3LYP/6-31G(d) optimized structures of poly(butyl- α -cyanoacrylate) tetrameric oligomers corresponding to eight tetrads (Scheme 2) as following: SSRS (*rrr*), SRSS (*mrm*), RRSS (*rrm*), SRSR (*mrr*), RRRS (*rmr*), SRRS (*mmr*), RRRR (*mmm*), SRRR (*mmm*). The terminology *R* or *S* refers to the convention of Cahn–Ingold–Prelog

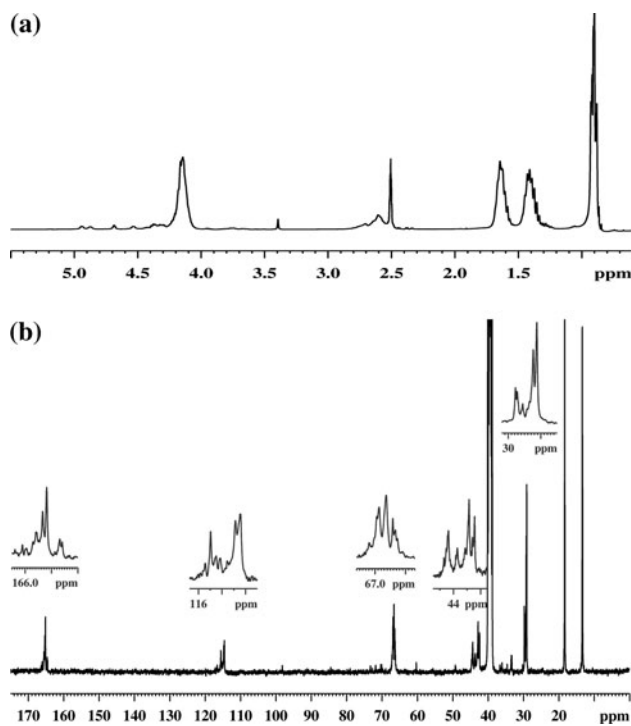
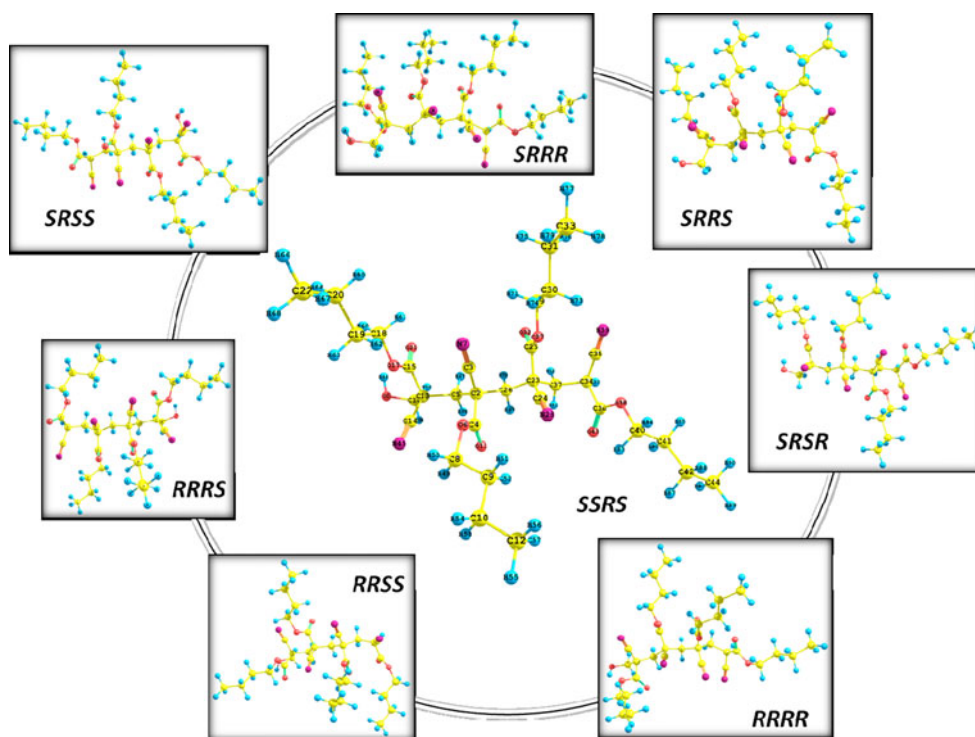


Fig. 2 **a** ^1H and **b** ^{13}C NMR spectra of PBCN in $\text{DMSO}-d_6$

HSQC, and $^1\text{H}/^{13}\text{C}$ HMBC techniques. Three main signals were observed in the spectral region of the side chain methylene protons (OCH_2 , 66 ppm). According to data published in the literature [26], it was suggested that the OCH_2 resonances of *mm* triads appear at higher field and

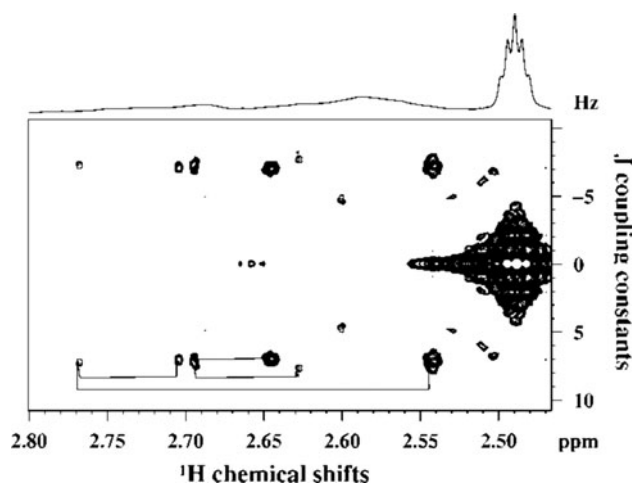


Fig. 3 Selected spectral area from 400.13 MHz ^1H J -resolved spectrum of PBCN

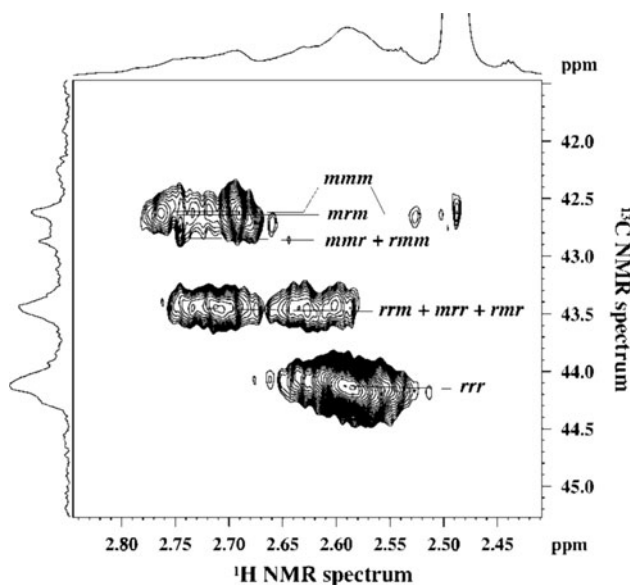
those of *rr* triads at lower field with respect to *rm* sequences. This result was further supported by the quantitative estimation of the stereochemical distribution of the monomer units in PBCN. The resonance signal of the methylene protons from the main polymer chains was used to analyze the tetrad arrangement of the polymer chains. The assignment was achieved by analysis of the $^1\text{H}/^{13}\text{C}$ HSQC spectra and the results are presented in Table 1 with the theoretical ^{13}C chemical shifts calculated. In the HSQC spectrum, four sets of cross-peaks appeared due to the interaction of methylene carbon and directly

Table 1 Bernoullian statistics for the tacticity of the side-chain and experimental ^{13}C chemical shifts for poly(butyl- α -cyanoacrylate) nanoparticles

Tacticity	Distribution at $P_m = 0.30$		^{13}C chemical shifts	
	Predicted	Observed	Exptl.	Calculated C26
Triads				
<i>rr</i>	0.49	0.48	66.65	
<i>mr + rm</i>	0.42	0.33	66.40	
<i>mm</i>	0.09	0.19	66.15	
Tetrads				
<i>rrr</i>	0.34	0.62	44.13	52.39
<i>rrm + mrr + rmr</i>	0.44	0.22	43.46	52.12
<i>mmr + rmm</i>	0.13	0.04	42.87	51.94
<i>mmm + mrm</i>	0.09	0.11	42.64	51.39

The GIAO BPW91/6-31+G(2d,p) calculated methylene ^{13}C chemical shifts are for poly(methyl- α -cyanoacrylate) tetramers. The numbering of the nuclei is shown on Fig. 1

P_m probability of meso placement

**Fig. 4** Selected spectral area from $^1\text{H}/^{13}\text{C}$ HSQC NMR spectrum of PBCN

attached protons in monomer sequences with different configurations.

In the *rrr* and *mrm* tetrads which are C_2 symmetric with respect to the main-chain methylene, the attached protons exhibit a singlet and the respective ^{13}C signals were easily defined (Fig. 4; Table 1). The cross-peak at 2.58/44.13 and 2.69/42.60 ppm were assigned to methylene group in *rrr* and *mrm* tetrads, respectively. The methylene protons in the other possible tetrads are non-equivalent and

appearance of two different resonance peaks (cross-peaks in $^1\text{H}/^{13}\text{C}$ HSQC spectra) were observed with variation in the chemical shift difference for the different sets. The set of cross-peaks in the spectral area 2.60–2.77/43.46 and 2.60–2.77/42.87 ppm were assigned to the interactions between methylene carbon and protons in *rrm*, *mrr*, and *rmr*, and those in *mmr* and *rmm* tetrads, respectively. The carbon resonance at 42.68 ppm was found to give one bond spin–spin coupling to the methylene protons at 2.50 and 2.73 ppm. This carbon resonance was assigned to the *mmm* tetrad in agreement with the theoretical calculated chemical shifts of the methylene carbons from the main polymer chains and data published in the literature for homopolymer with similar structures [27, 28].

The sequence distribution of the PBCN was estimated by quantitative analysis of their ^{13}C DEPT NMR spectra, to avoid the overlap between the resonance signals of the methylene and quaternary carbons from the main polymer chains. The mole fractions of the different triad and tetrad sequences included into the polymer structure were determined from the relative peak intensities of the carbon resonances of OCH_2 from the side chain and CH_2 from the main polymer chains, respectively. In the ^{13}C NMR spectrum, the resonances of the triad and tetrad sequences partly overlap, thus hampering the quantitative determination of the respective triad and/or tetrad populations in the polymer chains by direct integration of ^{13}C resonance signals. Therefore, the relative intensities of the carbon resonance signals in DEPT spectrum were obtained by deconvolution of the spectral lines using the standard Bruker software and Lorentzian curves. By analysis of the oxymethylene range (66.0–67.0 ppm) and methylene range (42.0–45.0 ppm), information about the triad and tetrad populations, respectively, was obtained. The relative triad and tetrad sequences distributions in PBCN based on the quantitative analysis of the ^{13}C DEPT NMR spectrum and those predicted, assuming a probability of the meso placement (P_m) of 0.30 according to the Bernoullian statistics [15] are presented in Table 1. In the statistically random Bernoullian model, the mole fractions (F) of each triad and tetrad can be calculated from the P_m value (0.30) assumed, according the following formulas:

$$F_{rr} = (F_r)^2 \quad F_{rm} = F_{mr} = F_r \cdot F_m \quad F_{mm} = (F_m)^2$$

$$F_{rrr} = (F_r)^3 \quad F_{mmm} = (F_m)^3$$

$$F_{rrm} = F_{mrr} = F_{rmr} = (F_r)^2 \cdot F_m$$

$$F_{mmr} = F_{rmm} = F_{mrm} = (F_m)^2 \cdot F_r$$

A significant deviation of the experimental data from those predicted by the Bernoullian statistics was observed, especially for the tetrads sequence distribution. The Bernoullian model predicts higher overall population of

Table 2 Total energy differences, ΔE_T (kcal mol⁻¹), of the poly(butyl- α -cyanoacrylate) tetramer structures, shown on Fig. 1, optimized at PM3 and B3LYP/6-31G(d) levels

Tetramer	PM3	B3LYP/ 6-31G(d)	BPW91/6-31+G(d)// B3LYP/6-31G(d)	
			Gas phase	DMSO
SSRS	5.05	0.00	0.00	0.00
SRRR	0.00	8.60	10.76	6.91
SRSS	2.07	8.75	9.93	3.03
RRRS	2.97	4.32	7.97	4.65
RRSS	1.73	3.31	7.71	6.11
SRRS	3.74	5.55	4.61	3.00
RRRR	1.80	7.78	5.31	3.27
SRSR	3.21	4.16	9.43	6.00

tetrads composed of stereochemically different monomer units (*rrm*, *mrr*, *rmr*, *mmr*, *rmm*, *mrmm*) with respect to those composed of stereochemically equal units (*rrr*, *mmm*). As expected, the *rrr* tetrads dominates over the *mmm* tetrads population for the assumed probability of meso placement ($P_m = 0.30$). In contrast to the predicted data, the experimental data show significantly lower overall population of tetrad sequences composed of stereochemically different monomer units with a predominance of the fraction of *rrr* tetrads (Table 1). The simplest random polymer model (Bernoullian model) cannot describe the sequence distribution in the polymer studied, which is an indication of a non-random arrangement of monomer units with different stereochemical configurations. In addition, the experimental results show that *rrr* is the preferred stereochemical sequence distribution of the monomer units in the homopolymer chains of PBCN.

The stereochemical distribution of the monomer units was additionally analyzed according the method suggested by Kamiya et al. [29]. The parameter D , ($D = rr\cdot mm / rm\cdot mr$), was used to characterize the distribution of the stereochemically different monomer units of PBCN. The value of the parameter D is dependent on the mole fractions of the triad present in the polymer and therefore related to the polymer tacticity. Polymers with randomly distributed monomer units have $D = 1$. Values of D higher than 1, suggest block-monomer distribution of the polymer structures and values smaller than 1 are characteristic of an alternating polymer. The parameter D was calculated to 3.35 for the PBCN obtained by the anionic polymerization and the existence of block stereosequence distribution with most favorable *rr* and *rrr* arrangement of the monomer units was assumed. The domination of the *rrr* tetrad fraction and high D value obtained for PBCN seems to reflect the preferred tendency for syndiotactic arrangement of the monomer units with ester ($-\text{COO}Bu$) and cyano groups

($-\text{CN}$) positioned on alternating sides of the main hydrocarbon backbone of poly(butyl- α -cyanoacrylate).

The tetramer of poly(butyl- α -cyanoacrylate) was chosen for the study as it is representative of the main population of the oligomers formed during the anionic polymerization process [30]. In this study, we tend to adopt a helical conformation with a radial display of the cyano and ester moieties around the carbon–carbon backbone (Fig. 1). The absolute configuration of the eight diastereoisomeric species of the poly(butyl- α -cyanoacrylate) is only considered. The ester ($-\text{COO}Bu$) and cyano groups ($-\text{CN}$) position around carbon–carbon backbone is substantial for nanoparticles producing but not a conformational behavior of the poly(butyl- α -cyanoacrylate). That is why we do not consider the PBCN conformers.

The values of the total energies differences (ΔE_T) for eight diastereoisomers configuration of poly(butyl- α -cyanoacrylate) obtained at PM3 and B3LYP/6-31G(d) levels are given in Table 2. According to our calculations using the semiempirical PM3 method, the most stable tetramer structure of poly(butyl- α -cyanoacrylate) is SRRR (*mmm* tetrad). The same result was observed by Poupaert and Couvreur [31]. The RRSS (*rrm*) and RRRR (*rmm*) tetramers of *n*-BCAis next in energy sequence; the ΔE_T difference values amounted to 1.73 and 1.80 kcal mol⁻¹, respectively, in favor of SRRR (*mmm*). However, when the electron correlation is taking into account at B3LYP/6-31G(d) level the most stable structure becomes the SSRS (*rrr*) one. The energy difference ΔE_T between most stable tetramers, SSRS and RRSS increases to 3.31 kcal mol⁻¹. According to energy differences obtained at single point BPW91/6-31+G(d)//B3LYP/6-31G(d) calculations in gas phase and DMSO solution, the SSRS structure is most stable again. However, energy differences between different tetramer structures decrease in DMSO solution.

It is well known that DFT often gives calculated magnetic shieldings in large systems of a quality comparable or even better than MP2 for a cost that is on the same order as Hartree–Fock, substantially less than that of traditional correlation techniques [32–34]. Exchange–correlation functionals are believed to be superior in predicting molecular properties [35–37]. We carried out calculations using B3LYP, OLYP, OPBE, BPW91, and B3PW91 functionals, and found the BPW91 results to be closest to experimental data. Therefore, we present only the BPW91 results in GIAO NMR calculations in DMSO. Because of the sensitivity of ¹³C NMR chemical shifts to the presence of polarization and diffuse functions in the basis set the 6-31+G(2d,p) basis set was employed [37, 38].

¹³C NMR chemical shifts were performed for tetramers of poly(methyl- α -cyanoacrylate) because of calculation reasons. We have made the GIAO NMR calculations for poly(methyl- α -cyanoacrylate) on the basis of replacement

of the butyl moiety by a methyl one in the optimized poly(butyl- α -cyanoacrylate). This replacement does not change the ^{13}C NMR chemical shifts of the polymer. The NMR predicted values of C26 chemical shifts were found to show the same dependence as experimental results. The higher value was obtained for nucleus C26 of the SSRS tetramer (*rrr* tetrad) of poly(methyl- α -cyanoacrylate) and the values of the rest of the tetramers decrease in parallel with the decrease in the experimentally obtained chemical shifts. They are presented in Table 1. The higher values of the chemical shifts for nucleus C26 could be explained by the fact that they were calculated for tetramers only, while the experimental ^{13}C NMR chemical shifts were obtained for octamers and longer polymer chains. Generally, quantum chemical analysis shows the SSRS tetramer (*rrr* triad) of *n*-BCA as most favorable structure for PBCN building as well as NMR observation.

Conclusions

The structural characterization and preferred stereochemical sequence distribution of the monomer units in the homopolymer chains of PBCN were estimated by ^1H and ^{13}C NMR spectroscopy (one- and two-dimensional techniques) and quantum chemical calculation. The values of the triad and tetrad populations were determined from the relative peak intensities of the carbon resonances of OCH_2 from the side chain and CH_2 from the main polymer chains, respectively. The results are consistent with the preferred tendency of polymer chains of PBCN to adopt syndiotactic placements. A combined NMR and quantum chemical investigations elucidate on the structure of poly(butyl- α -cyanoacrylate) and show that the most favorable tetramer in PBCN should be SSRS one (*rrr* triad).

Acknowledgments Funding of this study by the Bulgarian Fund for Scientific Research, under Grant DO 02-168/2008 is gratefully acknowledged. The quantum chemical calculations were performed on the computer system installed at the Institute of Organic Chemistry, Bulgarian Academy of Sciences with the financial support of the Bulgarian Scientific Research Fund under the Project “MADARA” (RNF 01/0110, contract no. DO 02-52/2008). The NMR spectrometers are part of the National NMR Network and were purchased in the framework of the National Programme for Scientific Re-equipment, contract REDE/1517/RMN/2005, with funds from POCI 2010 (FEDER) and Fundação para a Ciência e a Tecnologia (FCT). The authors are grateful to Dr N. Vasilev, Institute of Organic Chemistry, Bulgarian Academy of Sciences, Sofia for helpful discussions.

References

- Murday JS, Siegel RW, Stein J, Wright JF (2009) Biol Med 5:251–273
- Moghimi SM, Hunter AC, Murray JC (2005) FASEB J 19:311–330
- Wagner V, Dullaart A, Bock A-K, Zweck A (2006) Nat Biotechnol 24:1211–1217
- Couvreur P, Kante B, Roland M, Guiot P, Baudhuin P, Speiser P (1979) J Pharm Pharmacol 31:331–332
- Lenaerts V, Couvreur P, Christians-Leyh D, Joiris E, Rolland M, Rollman B, Speiser P (1984) Biomaterials 5:65–68
- Lye D, Couvreur P, Lenaerts V, Roland M, Speiser P (1984) Labo-Pharma 32:100–104
- Scherer D, Robinson JR, Kreuter J (1994) Int J Pharm 101:303–307
- Duncan R (1986) CRC Crit Rev Biocompat 2:127–145
- O'Sullivan C, Birkinshaw C (2002) Polym Degrad Stab 78: 7–15
- Muller RH, Lherm C, Herbolt J, Couvreur P (1990) Biomaterials 11:590–595
- Vansnick L, Couvreur P, Christiaens-Ley D, Roland M (1985) Pharm Res 1:36–41
- Lehrm C, Muller R, Puisieux F, Couvreur P (1992) Int J Pharm 84:13–22
- Leonard F, Kulkarni RK, Brandes G, Nelson J, Cameron JJ (1996) J Appl Polym Sci 10:259–272
- Shalaby SW, Shalaby WSW (2004) In: Shalaby SW, Burg KJL (eds) Absorbable and biodegradable polymers, Chap 5. CRC Press, Boca Raton, pp 59–75
- Tonelli AE (1989) NMR spectroscopy and polymer microstructure: the conformational connection. Wiley, New York
- Stewart JJP (1989) J Comput Chem 10:209–220
- Becke AD (1993) J Chem Phys 98:5648–5650
- Lee CT, Wang WT, Pople RG (1988) Phys Rev B 37:785–789
- Granovsky AA, Firefly version 7.1.G, <http://classic.chem.msu.ru/gran/firefly/index.html>
- Ditchfield R (1974) Mol Phys 27:789–807
- Wolinski K, Hilton JF, Pulay P (1990) J Am Chem Soc 112: 8251–8260
- Perdew JP, Wang Y (1992) Phys Rev B 45:13244–13249
- Frisch MJ, Trucks GW, Schlegel HB, Scuseria GE, Robb MA, Cheeseman JR, Scalmani G, Barone V, Mennucci B, Petersson GA, Nakatsuji H, Caricato M, Li X, Hratchian HP, Izmaylov AF, Bloino J, Zheng G, Sonnenberg JL, Hada M, Ehara M, Toyota K, Fukuda R, Hasegawa J, Ishida M, Nakajima T, Honda Y, Kitao O, Nakai H, Vreven T, Montgomery JA Jr, Peralta JE, Ogliaro F, Bearpark M, Heyd JJ, Brothers E, Kudin KN, Staroverov VN, Kobayashi R, Normand J, Raghavachari K, Rendell A, Burant JC, Iyengar SS, Tomasi J, Cossi M, Rega N, Millam JM, Klene M, Knox JB, Cross JB, Bakken V, Adamo C, Jaramillo J, Gomperts R, Stratmann RE, Yazyev O, Austin AJ, Cammi R, Pomelli C, Ochterski JW, Martin RL, Morokuma K, Zakrzewski VG, Voth GA, Salvador P, Dannenberg JJ, Dapprich S, Daniels AD, Farkas O, Foresman JB, Ortiz JV, Cioslowski J, Fox DJ (2009) GAUSSIAN 09, Revision A.01, Gaussian, Inc., Wallingford
- Murthy RSR, Reddy LH (2006) Poly(alkylcyanoacrylate) nanoparticles for delivery of anti-cancer drugs. In: Mansoor MA (ed) Nanotechnology for cancer therapy. Taylor & Francis Group, LLC, New York, pp 251–288
- Gnanou Y, Fontanille M (2008) Organic and physical chemistry of polymers. Wiley, Hoboken, p 29
- Suchoparek M, Spevacek J (1993) Macromolecules 26:102–106
- Robello DR, Eldridge TD, Michaels FM (1999) J Polym Sci A 37:2219–2224
- Dong L, Hill DJT, O'Donnell JH, Whittaker AK (1994) Macromolecules 27:1830–1834
- Kamiya N, Yamamoto Y, Inoue Y, Chujo R, Doi Y (1989) Macromolecules 22:1676–1682
- Beham N, Birkinshaw C, Clarke N (2001) Biomaterials 22:1335–1344
- Poupaert JH, Couvreur P (2003) J Control Release 92:19–26

32. Ochsenfeld C, Kussmann J, Koziol F (2004) *Angew Chem Int Ed* 43:4485–4489
33. Kussmann J, Ochsenfeld C (2007) *J Chem Phys* 127:204103
34. Beer M, Ochsenfeld C (2008) *J Chem Phys* 128:221102
35. Facelli JC (2011) *Prog NMR Spectroscopy* 58:176–201
36. Cheeseman JR, Trucks GW, Keith TA, Frisch MJ (1996) *J Chem Phys* 104:5497–5509
37. Blicharska B, Kupka T (2002) *J Mol Struct* 613:153–166
38. d'Antuono P, Botek E, Champagne B, Wiem J, Reyniers M-F, Marin GB, Adriaensens PJ, Gelan JM (2005) *Chem Phys Lett* 41:207–213